Theoretical efficiency of solar thermoelectric energy generators

Citation: Chen, Gang. "Theoretical Efficiency of Solar Thermoelectric Energy Generators." Journal of Applied Physics 109.10 (2011): 104908. ©2011 American Institute of Physics

As Published: http://dx.doi.org/10.1063/1.3583182

Publisher: American Institute of Physics (AIP)

Persistent URL: http://hdl.handle.net/1721.1/78245

Version: Final published version: final published article, as it appeared in a journal, conference proceedings, or other formally published context

AIP | Journal of Applied Physics

Theoretical efficiency of solar thermoelectric energy generators

Gang Chen

Citation: J. Appl. Phys. 109, 104908 (2011); doi: 10.1063/1.3583182
View online: http://dx.doi.org/10.1063/1.3583182
View Table of Contents: http://jap.aip.org/resource/1/JAPIAU/v109/i10
Published by the American Institute of Physics.

Theoretical efficiency of solar thermoelectric energy generators

Gang Chen[a)]
Mechanical Engineering Department, Massachusetts Institute of Technology, Cambridge, Massachusetts 02139, USA

(Received 28 December 2010; accepted 4 March 2011; published online 20 May 2011)

This paper investigates the theoretical efficiency of solar thermoelectric generators (STEGs). A model is established including thermal concentration in addition to optical concentration. Based on the model, the maximum efficiency of STEGs is a product of the opto-thermal efficiency and the device efficiency. The device efficiency increases but the opto-thermal efficiency decreases with increasing hot side temperature, leading to an optimal hot-side temperature that maximizes the STEG efficiency. For a given optical concentration ratio, this optimal hot-side temperature depends on the thermoelectric materials' nondimensional figure-or-merit, the optical properties of wavelength-selective surface and the efficiency of the optical system. Operating in an evacuated environment, STEGs can have attractive efficiency with little or no optical concentration working in the low temperature range (150–250 °C) for which Bi_2Te_3-based materials are suitable. © *2011 American Institute of Physics*. [doi:10.1063/1.3583182]

I. INTRODUCTION

The conversion of solar energy into electricity has so far focused on two approaches.[1] One is solar photovoltaic (PV) that converts photon energy into electricity via electron-hole pair generation. The other is solar-thermal that converts photon energy into a terrestrial heat source, usually through optical concentrators, and uses mechanical heat engines to generate electricity.[2,3] Besides mechanical heat engines, a terrestrial heat source created from the solar energy can also be coupled to a thermoelectric device to generate electricity. Thermoelectric power generation relies on the Seebeck effect in solid materials to convert thermal energy into electricity.[4,5] In solar-thermal systems, by replacing the mechanical heat engines with thermoelectric generators, solid-state solar-thermal to electricity energy conversion is possible. Being a solid-state technology, such solar thermoelectric generator (STEG) cells share many advantages similar to PV cells.

The prospect of converting solar energy first into a terrestrial heat source and then into electricity via thermoelectric generators was realized shortly after the discovery of the Seebeck effect. Until recently, solar thermoelectric energy conversion had yielded low efficiencies, and had not drawn much attention. Telkes[6] gave a brief summary of the work in STEGs before 1954, and reported STEGs constructed of ZnSb and Bi-Sb alloys. The maximum efficiency achieved of a flat-panel STEG was 0.63%. Under 50 times optical concentration, the efficiency reached 3.35%. However, these efficiencies may be inaccurate; Telkes used the average regional solar flux (800 W/m^2) to calculate efficiency, and not the actual incident flux. Few papers have been published on STEGs since Telkes' report. Rush[7] investigated a flat-panel STEG configuration for space applications with an estimated maximum efficiency of 0.7%. Goldsmid *et al.*[8] carried out experiments on STEGs using both flat-panel and optically concentrated configurations. For the flat-panel configuration, the reported generator efficiency is ~1.4% but the system efficiency is only ~0.6% due to radiation and conduction losses, comparable to that of Telke's report. Under ~4 times optical concentration, their reported system efficiency decreased to 0.5% due to optical losses. Dent and Cobble[9] used a sun-tracking heliostat directing the solar radiation on a parabolic dish, which focused the sunlight onto thermoelectric generators using PbTe thermoelectric elements. A thermodynamic efficiency of 4% was estimated when the hot side was heated to 510 °C, based on the calculated heat input to the thermoelectric generators. Considering the optical concentration losses, the system efficiency of Dent and Cobble's generator at best would be similar to that of Telkes. A recent experimental study[10] on STEG with ~6 ×concentration and thermoelectric module reported only 0.15% efficiency. Under 66× solar concentration, Amatya and Ram reported a system efficiency of 3% using commercial Bi_2Te_3-based thermoelectric generators,[11] similar to that of Telkes.[6]

There are a few modeling studies on solar thermoelectric generations. Telkes[6] included air conduction and convection heat losses in analyzing the STEG cell performance. She treated radiation loss by an effective convection heat transfer coefficient. These analyses are valid only when the temperature rise on the absorber is small. A modeling study[12] on STEGs reported an efficiency of 50%, which is higher than what is theoretically possible from an ideal thermoelectric generator using parameters given in the paper, casting serious doubt on the validity of the analysis in the paper. Novikov[13] gave an analysis on STEGs including 4th power law of thermal radiation, but only numerical results were presented. It is not clear from this study what parameters are important in determining the maximum system efficiency. Several papers have analyzed STEGs for spacecraft applications, focusing on near-Sun orbitals where the solar flux is large.[14–17] For space applications, one advantage is that the convection

a)Electronic mail: gchen2@mit.edu.

loss is eliminated. However, heat rejection at the cold side can occur only via thermal radiation, which is inefficient and limits the overall system efficiency.

Based on the above discussion, we conclude that there exists no systematic analysis of the potential performance of STEG cells under terrestrial operation condition. This paper presents an analysis of the potential performance of STEG cells for terrestrial applications. Our emphasis is placed on evacuated systems, although the formulation presented includes the case for atmospheric operation. Existing technologies in evacuated tubes for solar-thermal steam plant and solar hot-water systems have proven that vacuum operations are realistic and economically feasible.[18] We found that ~5% or higher system efficiencies can be achieved using evacuated STEG cells with little or no optical concentration. This prediction is consistent with our recent experimental demonstration.[19] The analysis presented here point to one fruitful direction for future research in converting solar energy into electricity.

II. MATHEMATICAL MODELS

We consider a unit cell of a generic STEG as shown in Fig. 1. A wavelength-selective surface, which will be called a selective surface, of area A_s absorbs the solar radiation and hence raises its temperature. The selective surface is coupled to the hot side of a pair of p-type and n-type thermoelectric elements that generate electricity. The selective surface is designed such that it has a high absorptance to solar radiation but a low emittance at its operational temperature.[20] Solar radiation with an insolation q_s is directed toward the selective surface, with or without optical concentration. When optical concentration is used, via either imaging or nonimaging methods,[21] it is assumed that the selective surface area is equal to the focal area of the optical system, and that the optical concentration ratio γ_{op} is defined as the ratio of the cross-sectional area of the aperture of the optical system divided by the frontal area of the selective surface. In this study, the selective surface is assumed to be flat and hence the frontal area equals to actual area. As incoming solar radiation is absorbed by the selective surface, heat is conducted along the selective surface to the thermoelectric elements.

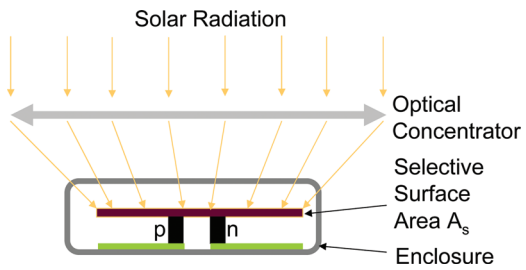

FIG. 1. (Color online) Illustration of the unit cell of a STEG modeled in this work. Solar radiation may go through an optical concentrator with a concentration ratio γ_{op} and efficiency η_{op}, transmit through a glass enclosure with a transmittance τ_g, and be absorbed by a wavelength-selective surface with a solar absorptance α_s and effective thermal emittance ε_c. Heat absorbed conducts through thermoelectric elements and is dissipated to the environment at the cold side. Thermal concentration γ_{th} is the ratio of the selective surface area A_s divided by the total cross-sectional area of the p-type and the n-type thermoelectric elements.

This process is called thermal concentration and the thermal concentration ratio γ_{th} is defined as the area of the selective surface divided by the cross-sectional area of the thermoelectric generator, which we also assume equals to the ratio of the selective-surface area for one unit cell and cross-sectional area of one pair of p-n thermoelectric elements. In addition to conduction into the thermoelectric elements, heat absorbed by the selective surface is also lost from the hot selective surface to the ambient via (1) radiation to the surroundings at a temperature T_a, (2) radiation to the cold side radiation shield at temperature T_c, and (3) conduction and convection loss if the STEG is not in a vacuum. We further make the following approximations:

(1) The selective surface is maintained at a uniform temperature T_h, which is also the hot side temperature of the thermoelectric elements. This approximation can be justified readily for many cases by a simple heat transfer analysis using a fin model with internal heat generation along the fin due to the absorbed solar radiation.[22]

(2) The thermoelectric properties are independent of temperature. While real materials' thermoelectric properties are all temperature dependent, the assumption of temperature independent properties will allow identification of key nondimensional parameters affecting the system performance.[4] Analysis based on temperature dependent properties will be presented in the future.

(3) Electrical and thermal contact resistances are negligible. The importance of electrical and thermal contact resistances are well recognized in thermoelectric device literature.[4] This approximation is made to allow us focusing on predicting the best performance of the STEGs.

Applying energy balance to the selective surface, we have

$$\gamma_{op}\tau_g\alpha_s\eta_{op}q_sA_s = Q_{te} + \varepsilon_{sa}\sigma A_s\left(T_h^4 - T_a^4\right) + \varepsilon_{sc}\sigma(A_s - A_{te})\left(T_h^4 - T_c^4\right) + Q_{con}, \quad (1)$$

where q_s is the solar insolation per unit area, Q_{te} is the heat flow from the thermoelectric elements to the cold side, Q_{con} represents the conduction and convection loss if the enclosure is not evacuated, η_{op} the optical concentration efficiency, τ_g is the transmittance of the glass enclosure, α_s the absorptance of the selective surface to the solar flux, ε_{sa} the emittance between the selective surface and the ambient at the operation temperature of the selective surface, ε_{sc} the effective emittance between the selective absorber and the cold side. Both ε_{sa} and ε_{sc} can be further modeled based on the arrangements of the selective surface relative to its surroundings, although we will assume that ε_{sa} is simply the property of the selective surface itself and ε_{sc} can be calculated using the results of radiation heat transfer between two parallel surfaces,[23]

$$\varepsilon_{sc} = \frac{1}{1/\varepsilon_h + 1/\varepsilon_c - 1} \quad (2)$$

in which one surface is the back side of the selective absorber with an emittance of ε_h and the other the cold side with an emittance ε_c. We have neglected in Eq. (1) the heat loss from the side walls of thermoelectric elements. To

simplify the analysis, we further assume that the cold side T_c is the same as the ambient temperature T_a.

For a gas filled enclosure, the conduction and convection loss can be expressed as

$$Q_{con} = \left[k_{air}\frac{(A_s - A_n - A_p)}{L} + \frac{1}{R_{con1}}\right](T_h - T_c) = \frac{T_h - T_c}{R_{con}}, \tag{3}$$

where R_{con1} is the heat conduction loss from the top side of the selective surface to the ambient. We neglect surface area A_{te} in the right hand side of Eq. (1) and thus can combine the two radiation loss term with an effective emittance $\varepsilon_e (= \varepsilon_{sa} + \varepsilon_{sc})$, such that Eq. (1) becomes

$$\gamma_{op}\tau_g\alpha_s\eta_{op}q_sA_s = Q_{te} + \varepsilon_e\sigma A_s(T_h^4 - T_c^4) + \frac{T_h - T_c}{R_{con}}. \tag{4}$$

The approximations we made so far mean that our model will become less accurate as the area of the selective surface becomes comparable to that of the cross-sectional area of the thermoelectric elements, i.e., when the optical concentration is large and thermal concentration is small.

Heat leaving the selective surface via the thermoelectric elements can be expressed as[4]

$$Q_{te} = (S_p - S_n)T_hI + \frac{(T_h - T_c)}{R_{tp} + R_{tn}} - \frac{1}{2}I^2(R_{ip} + R_{in}), \tag{5}$$

where I is the current flowing through the thermoelectric n-type and p-type elements, S_p and S_n are the Seebeck coefficients of the p-type and the n-type thermoelectric materials, respectively, R_{tp} and R_{tn} their corresponding thermal resistances, and R_{ip} and R_{in} their corresponding electrical resistances, which are related to thermal conductivity k, electrical resistivity ρ through

$$R_{tp} = \frac{k_pA_p}{L_p}, \quad R_{tn} = \frac{k_nA_n}{L_n}, \tag{6}$$

$$R_{ip} = \frac{\rho_pA_p}{L_p}, \quad R_{in} = \frac{\rho_nA_n}{L_n}, \tag{7}$$

where A and L with subscripts p and n represents cross-sectional area and the length of the p-type and n-type thermoelectric elements, respectively. We further assume $L_n = L_p$, a condition that can be easily relaxed following the same procedures in the analysis.

The electrical power output of the thermoelectric elements is

$$\begin{aligned} P_e &= I\left[(S_p - S_n)(T_h - T_c) - I(R_{ip} + R_{in})\right] \\ &= I\left[S_{pn}(T_h - T_c) - IR_e\right], \end{aligned} \tag{8}$$

where $S_{pn} = S_p - S_n$. The efficiency of the STEG cell is then

$$\eta = \frac{P_e}{\gamma_{op}A_sq_s} = \frac{I\left[S_{pn}(T_h - T_c) - IR_i\right]}{\gamma_{op}A_sq_s}, \tag{9}$$

where $R_i = R_{in} + R_{ip}$ is the internal resistance of the thermoelectric elements. We can rewrite the above expression into

$$\eta = \frac{Q_{te}}{q_sA_s} \times \frac{P_{te}}{Q_{te}} = \eta_{ot}\eta_{te}, \tag{10}$$

where the first term represents how much of the incident solar energy is transferred into thermoelectric elements and is called the opto-thermal efficiency (η_{ot}), and the second term represents how much heat input to thermoelectric elements is converted into electricity and hence is the device efficiency. Conventional thermoelectric generators optimize external load (and hence current I) to maximum device efficiency η_{te}. However, for solar thermoelectric generations, the current I also causes the hot side temperature T_h to change, as suggested by Eqs. (1), (4), and (5). Consequently, it is not clear whether the optimal working conditions for stand-alone thermoelectric generators also maximize the efficiency of STEGs.

The STEG efficiency is a function of current (I), the hot side temperature (T_h), the selective absorber area (A_s) and its effective emittance (ε_e), thermoelectric element geometries (cross-sectional areas A_n, A_p, and length L), and their thermoelectric properties. To reduce the variables, we introduce

$$\gamma_{th,p} = \frac{A_s}{A_p}, \quad \gamma_{np} = \frac{A_n}{A_p}, \quad Y = \frac{IL}{A_p} \tag{11}$$

to rewrite the efficiency expression, Eq. (9), and energy balance Eq. (1) into

$$\eta = \frac{Y\left[S_{pn}(T_h - T_c) - Y\left(\rho_p + \rho_n/\gamma_{np}\right)\right]}{C\gamma_{th,p}L} \tag{12}$$

and

$$\begin{aligned} \tau_g\alpha_s\eta_{op}C\gamma_{th,p} = {} & S_{pn}T_h\frac{Y}{L} + \left(k_p + k_n\gamma_{np} + k_a\left(\gamma_{th,p} - 1 - \gamma_{np}\right)\right. \\ & \left. + \frac{\gamma_{th,p}L}{R''_{con1}}\right)\frac{T_h - T_c}{L} - \frac{Y^2}{2L}\left(\rho_p + \frac{\rho_n}{\gamma_{np}}\right) \\ & + \varepsilon_e\sigma\gamma_{th,p}\left(T_h^4 - T_c^4\right), \end{aligned} \tag{13}$$

where $C = q_i\gamma_{op}$ and $R''_{con1} = A_sR_{con1}$ is the specific thermal resistance from top of selective surface to the ambient.

III. MAXIMUM EFFICIENCY

We aim at maximizing the efficiency of Eq. (12), subject to the constraint, Eq. (13), by optimizing the hot side temperature and other parameters, including $\gamma_{th,p}$, γ_{pn}, L, and Y. We use the Lagrangian multiplier method. Details of the derivation are given in the Appendix. Main results will be summarized below.

First, we note that the STEG efficiency can be expressed as

$$\begin{aligned} \eta &= \eta_{ot}\eta_{te} \\ &= \left[\tau_g\alpha_s\eta_{op} - \frac{\varepsilon_e\sigma\left(T_h^4 - T_c^4\right)}{\gamma_{op}q_i}\right]\left[\frac{(T_h - T_c)}{T_h}\frac{\sqrt{1 + ZT_m} - 1}{\sqrt{1 + ZT_m} + T_c/T_h}\right], \end{aligned} \tag{14}$$

where T_m is the arithmetic mean temperature between T_h and T_c, and η_{ot} and η_{te} correspond to the first and second terms in the square brackets of the last equation. The device efficiency is identical to the maximum efficiency of a thermoelectric generator operating between T_h and T_c. However, unlike a regular thermoelectric generator that has different load matching conditions for the maximum efficiency and the maximum power, STEGs' maximum efficiency is also the maximum power point, and the load matching condition is

$$R_e/R_i = \sqrt{1+ZT_m}, \tag{15}$$

where R_i is internal resistance and R_e is external load resistance. This condition is identical to that of maximizing efficiency condition for a regular thermoelectric power generator, and it also maximizes the power output for STEGs. In contrast, the power of a regular thermoelectric generator is maximized when $R_e/R_i = 1$.

To achieve the maximum efficiency, the p and the n elements should have their cross-sectional areas matched to their properties according to

$$\gamma_{np} = \frac{A_n}{A_p} = \sqrt{\frac{\rho_n k_p}{\rho_p k_n}} \tag{16}$$

for equal element length L. This result is also identical to that obtained from analyzing one pair of ideal devices.[8]

The analysis given in the appendix also leads to

$$\frac{\tau_g \alpha_s \eta_{op} \gamma_{op} q_i - \varepsilon_e \sigma (T_h^4 - T_c^4)}{4\varepsilon_e \sigma T_h^4} = \frac{\sqrt{1+ZT_m}\left[\sqrt{1+ZT_m} + T_c/T_h\right]}{\left[T_c\sqrt{1+ZT_m}/(T_h - T_c) + 1/2\right]\left(\sqrt{1+ZT_m}+1\right)} \tag{17}$$

and

$$\gamma_{th,p} L = (k_p + k_n \gamma_{np}) \frac{T_c\sqrt{1+ZT_m} + (T_h - T_c)/2}{4\varepsilon_e \sigma T_h^3 T_m}. \tag{18}$$

Equation (17) gives the optimal hot-side operational temperature T_h and Eq. (18) the optimal thermal concentration ratio which equals $r_{th,p}/(1+\gamma_{np})$. What is interesting is that the optimal hot-side temperature T_h as determined from Eq. (17) does not depend on the thermal concentration ratio or element length. Once the optical properties and ZT_m are given, the optimal hot side temperature is fixed, and consequently, the best achievable efficiency. To arrive at such an optimal efficiency, the thermal concentration ratio and element length L should satisfy Eq. (18).

Figure 2 shows the device efficiency, η_{te}, the opto-thermal efficiency, η_{ot}, and the STEG system efficiency as a function of T_h, without any optical concentration at the AM1.5 condition ($q_s = 1000$ W/m^2). The opto-thermal efficiency decreases while the device efficiency increases with increasing operational temperature T_h, leading to a maximum efficiency at certain T_h. For materials with $ZT_m = 1$ and no optical concentration, the optimal temperature T_h is close to 150–250 °C, depending on values of the emittance.

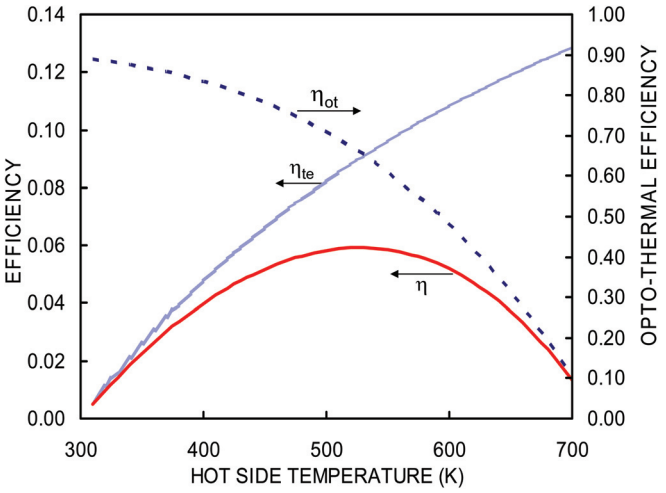

FIG. 2. (Color online) In a STEG cell, opto-thermal efficiency (η_{ot}) decreases while the thermoelectric generator efficiency (η_{te}) increases with increasing the hot-side temperature, leading to an optimal operational temperature that maximizes the system efficiency (η) ($ZT_m = 1$, $\varepsilon_e = 0.06$).

This is interesting because best known thermoelectric materials, Bi_2Te_3 and its alloys, can be used for this temperature range,[4,5] and good progress has been made in these materials' ZT values via nanostructuring.[24–27]

Figure 3(a) shows the maximum efficiency as a function of ZT_m for different optical concentration ratios γ_{op}, and Figs. 3(b) and 3(c) the corresponding hot side temperature and the thermal concentration $\gamma_{th,p}/(1+\gamma_{np})$, by taking $L = 1$ mm in Eq. (18). Figures 3(b) and 3(c) shows that a large thermal concentration can be used to create the needed temperature difference to drive the thermoelectric generator in the absence of any optical concentration. For example, at $ZT_m = 1$ and $\gamma_{op} = 1$, thermal concentration as large as 700–800 should be used (for $L = 1$ mm) and a system efficiency 5–6% is possible. The advantage of thermal concentration is that it can be achieved in a flat-panel configuration, in contrast to complicated and bulky optical concentration systems, enabling STEGs with a form factor comparable to photovoltaic cells. The large thermal concentration also means that only small amount of thermoelectric materials is needed. Shorter thermoelectric elements lead to a reduction in the thermoelectric materials required not only via directly reducing the materials, but also via increasing the thermal concentration ratio. Of course, practically, the electrical contact resistance and the temperature drop in both the selective surface and the bottom heat spreader limits how small the element length can be.

For systems with no optical concentration, the radiation loss has significant impact on the STEG system efficiency. In Fig. 4(a), we show the effect of the emittance of the selective surface on the system efficiency. Reducing the emittance can have similar effect as increase ZT. Reducing the emittance also means that the STEGs can operate at higher temperatures [Fig. 4(b)] with even higher efficiencies due to the increasing device efficiency η_{te}.

We should caution, however, there is a fundamental limit regarding to achieving high solar absorptance and low emittance by the selective surface. An ideal selective surface

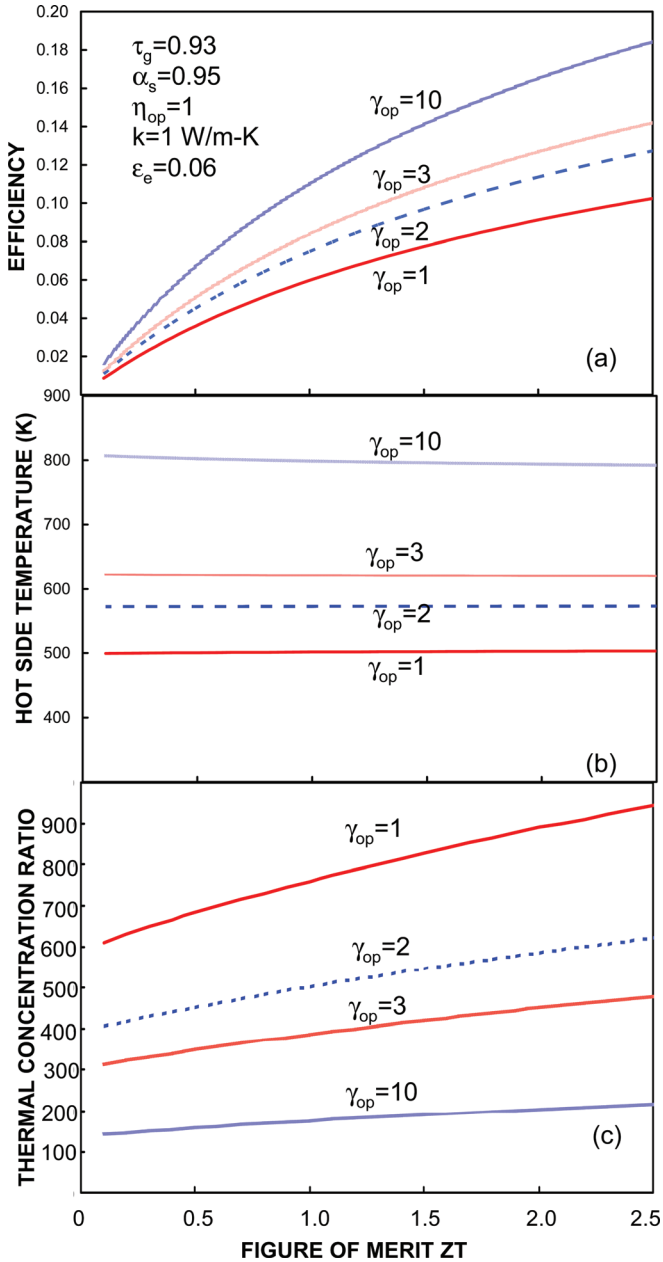

FIG. 3. (Color online) Dependence of (a) STEG efficiency, (b) hot-side temperature, and (c) thermal concentration, on the dimensionless figure-of-merit ZT for different optical concentrations. Other parameters are given in the figure. Thermoelectric element length is taken as 1 mm in the calculation of the thermal concentration.

should have an absorptance of 1 for most of the solar spectrum and an emittance of zero for the longer wavelength spectrum. We assume the solar radiation as a blackbody of temperature 5800 K. To achieve an absorptance of 0.95, the selective surface should absorb all solar radiation with a wavelength shorter than 2.17 μm. At this cut-off wavelength, the lowest emittance of the surface can be calculated based on the universal blackbody relation,[23] by assuming a zero emittance for photons with a wavelength longer than the cut-off wavelength. In Fig. 4(b), we also plot the emittance-temperature relation of such an ideal selective surface with a solar absorptance of 0.95. The temperature region above this curve cannot be achieved.

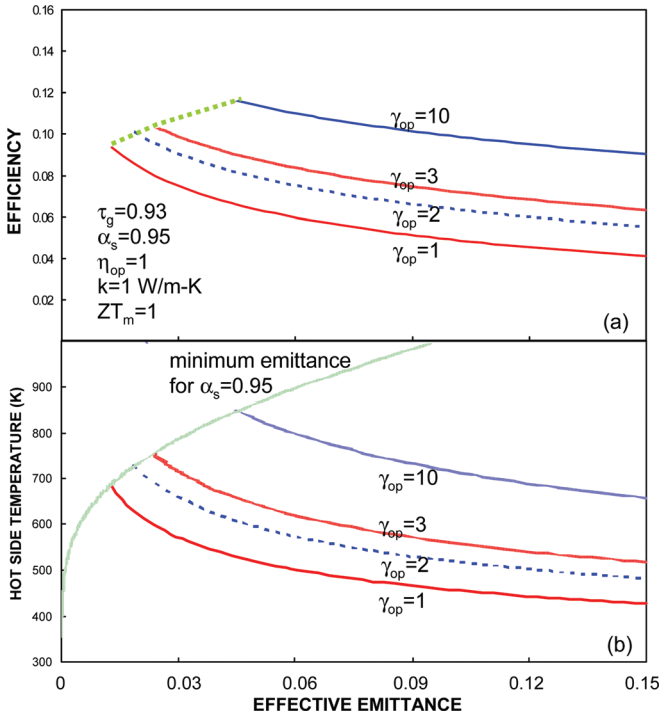

FIG. 4. (Color online) Dependence of (a) STEG efficiency, and (b) selective surface temperature on the effective emittance of the selective surface. Other parameters are given in the figure. The minimum emittance curve represents the lowest emittance that a selective surface can have at a 95% solar absorptance.

IV. SUMMARY

We have developed a model for STEGs and obtained the conditions leading to the maximum efficiency of STEGs. The efficiency of STEGs is a product of the thermal efficiency and the thermoelectric device efficiency. The former decreases while the latter increases with increasing selective surface temperature, leading to the existence of an optimal operational temperature that is dependent on the nondimensional figure-of-merit ZT_m and the optical properties of the system, but independent of the device geometry. It is also found that the product of the thermal concentration ratio and the thermoelectric element length should be a constant for a given ZT_m value and optical and thermal properties. Numerical results suggest that with little or no optical concentration, STEG system efficiency larger than 5% can be achieved with a hot-side operational temperature between 150–250 °C, which matches that of Bi_2Te_3-based materials and is consistent with our recent experiment. Due to the large thermal concentration, only small amount of thermoelectric materials are needed for STEGs, making them an attractive direction to pursue in harnessing solar energy into electricity.

ACKNOWLEDGMENTS

The author gratefully acknowledges fruitful discussions with Daniel Kraemer, Kenneth McEnaney, Andrew Muto, Dr. Bed Poudel, and Professor Zhifeng Ren, and thanks George Ni for proofreading the manuscript. This work is supported as part of the "Solid State Solar-Thermal Energy

Conversion Center (S^3TEC), an Energy Frontier Research Center funded by the U.S. Department of Energy, Office of Science, Office of Basic Energy Sciences under Award No. DE-SC0001299.

APPENDIX: DERIVATION OF MAXIMUM EFFICIENCY

To optimize the STEG efficiency, we use the Lagrangian multiplier method,

$$\eta(T_h, Y, L, \gamma_{th,p}, \gamma_{pn}) = \frac{Y\lfloor S_{pn}(T_h - T_c) - Y(\rho_p + \rho_n/\gamma_{np})\rfloor}{C\gamma_{th,p}L} + \lambda\left[\begin{array}{l} S_{pn}T_h\frac{Y}{L} + \left(k_p + k_n\gamma_{np} + k_a(\gamma_{th,p} - 1 - \gamma_{np}) + \frac{\gamma_{th,p}L}{R''_{con1}}\right)\frac{T_h - T_c}{L} - \frac{Y^2}{2L}\left(\rho_p + \frac{\rho_n}{\gamma_{np}}\right) \\ + \varepsilon_e\sigma\gamma_{th,p}(T_h^4 - T_c^4) - \tau_g\alpha_s\eta_{op}C\gamma_{th,p} \end{array}\right], \tag{A1}$$

$$0 = \frac{\partial\eta}{\partial\gamma_{th,p}} = -\frac{Y\lfloor S_{pn}(T_h - T_c) - Y(\rho_p + \rho_n/\gamma_{np})\rfloor}{C\gamma_{th,p}^2 L} + \lambda\left[\left(k_a + \frac{L}{R''_{con1}}\right)\frac{T_h - T_c}{L} + \varepsilon_e\sigma(T_h^4 - T_c^4) - \tau_g\alpha_s\eta_{op}C\right], \tag{A2}$$

$$0 = \frac{\partial\eta}{\partial\gamma_{np}} = \frac{Y^2\rho_n/\gamma_{np}^2}{C\gamma_{th,p}L} + \lambda\left[(k_n - k_a)\frac{T_h - T_c}{L} + \frac{Y^2}{2L}\left(\frac{\rho_n}{\gamma_{np}^2}\right)\right], \tag{A3}$$

$$0 = \frac{\partial\eta}{\partial Y} = \frac{S_{pn}(T_h - T_c) - 2Y(\rho_p + \rho_n/\gamma_{np})}{C\gamma_{th,p}L} + \lambda\left[S_{pn}T_h\frac{1}{L} - \frac{Y}{L}\left(\rho_p + \frac{\rho_n}{\gamma_{np}}\right)\right], \tag{A4}$$

$$0 = \frac{\partial\eta}{\partial T_h} = \frac{YS_{pn}}{C\gamma_{th,p}L} + \lambda\left[S_{pn}\frac{Y}{L} + \left(k_p + k_n\gamma_{np} + k_a(\gamma_{th,p} - 1 - \gamma_{np}) + \frac{\gamma_{th,p}L}{R''_{con1}}\right)\frac{1}{L} + 4\varepsilon_e\sigma\gamma_{th,p}T_h^3\right], \tag{A5}$$

$$0 = \frac{\partial\eta}{\partial L} = -\frac{Y\lfloor S_{pn}(T_h - T_c) - Y(\rho_p + \rho_n/\gamma_{np})\rfloor}{C\gamma_{th,p}L^2} + \lambda\left[-S_{pn}T_h\frac{Y}{L^2} - (k_p + k_n\gamma_{np} + k_a(\gamma_{th,p} - 1 - \gamma_{np}))\frac{T_h - T_c}{L^2} + \frac{Y^2}{2L^2}\left(\rho_p + \frac{\rho_n}{\gamma_{np}}\right)\right]. \tag{A6}$$

From Eqs. (A2) and (A6), together with the energy balance Eq. (13), we obtain

$$k_a\gamma_{th,p}\frac{T_h - T_c}{L} = 0. \tag{A7}$$

This equation implies in the case of conduction and convection heat loss via air, we should have L approaches infinite to maximize the efficiency. Hence, for a nonevacuated system, we should use long elements. Since optimizing this case is not interesting, we will next focus on evacuated system by setting $k_a = 0$ and R_{con1} approaches infinite in the above equations.

From Eqs. (A4) and (A6), we obtain,

$$Y = \frac{(k_p + k_n\gamma_{np})(T_h - T_c)\left(\sqrt{1 + S_{pn}^2T_m/[(\rho_p + \rho_n/\gamma_{np})(k_p + k_n\gamma_{np})]} - 1\right)}{S_{pn}T_m}, \tag{A8}$$

>where $T_m = (T_h + T_c)/2$ is the average temperature. It is clear that

$$ZT_m = S_{pn}^2T_m/[(\rho_p + \rho_n/\gamma_{np})(k_p + k_n\gamma_{np}) \tag{A9}$$

is the average ZT_m, and it is maximized when the two thermoelectric element cross-sectional area ratio matches to

$$\gamma_{np} = \frac{A_n}{A_p} = \sqrt{\frac{\rho_n k_p}{\rho_p k_n}}. \tag{A10}$$

This result is identical to that obtained from analyzing one pair of ideal devices.[8] Equation (A8) can be recast into

$$Y = \frac{(k_p + k_n\gamma_{np})(T_h - T_c)\left(\sqrt{1 + ZT_m} - 1\right)}{S_{pn}T_m}. \tag{A11}$$

From the above equation, we can show that the internal voltage drop across the pair of elements is

$$V_i = IR_i = \frac{S_{pn}(T_h - T_c)\left(\sqrt{1 + ZT_m} - 1\right)}{ZT_m} = \frac{S_{pn}(T_h - T_c)}{\sqrt{1 + ZT_m} + 1}, \tag{A12}$$

and consequently, the external voltage drop

$$V_e = S_{pn}(T_h - T_c) - V_i = \frac{S_{pn}(T_h - T_c)\sqrt{1+ZT_m}}{\sqrt{1+ZT_m}+1}. \quad \text{(A13)}$$

Equations (A12) and (A13) mean that the load matching condition

$$R_e/R_i = \sqrt{1+ZT_m} \quad \text{(A14)}$$

for the maximum efficiency in an ideal pair of thermoelectric device also applies to STEGs.

Substituting Y in Eq. (A11) into Eq. (12), we obtain

$$\eta = \frac{(k_p + k_n\gamma_{np})(T_h - T_c)^2\left(\sqrt{1+ZT_m}-1\right)\left[1-\left(\sqrt{1+ZT_m}-1\right)/(ZT_m)\right]}{C\gamma_{th,p}LT_m}. \quad \text{(A15)}$$

Examining the above equation, we see that we should also express $\gamma_{th,p}L$ in terms of Y. We use the energy balance Eq. (13) to get

$$\frac{(k_p + k_n\gamma_{np})}{\gamma_{th,p}L} = \frac{\tau_g\alpha_s\eta_{op}C - \varepsilon_e\sigma(T_h^4 - T_c^4)}{\left[S_{pn}T_hY - Y^2(\rho_p + \rho_n/\gamma_{np})/2\right]/(k_p + k_n\gamma_{np}) + (T_h - T_c)} = \frac{T_m\left[\tau_g\alpha_s\eta_{op}C - \varepsilon_e\sigma(T_h^4 - T_c^4)\right]}{(T_h - T_c)T_h\sqrt{1+ZT_m}\left[\sqrt{1+ZT_m} + T_c/T_h\right]/\left(\sqrt{1+ZT_m}+1\right)}. \quad \text{(A16)}$$

Combining Eqs. (A15) and (A16), we obtain

$$\eta = \frac{(T_h - T_c)}{T_h}\frac{\sqrt{1+ZT_m}-1}{\sqrt{1+ZT_m}+T_c/T_h}\left[\tau_g\alpha_s\eta_{op} - \frac{\varepsilon_e\sigma(T_h^4 - T_c^4)}{\gamma_{op}q_i}\right]. \quad \text{(A17)}$$

The above expression shows that efficiency can be split into the product of a opto-thermal efficiency and that of the efficiency of thermoelectric devices.

Next, we should find the equation that determines the optimal hot side temperature. From Eqs. (A4) and (A5)

$$\frac{S_{pn}(T_h - T_c) - 2Y(\rho_p + \rho_n/\gamma_{np})}{YS_{pn}} = \frac{\left[S_{pn}T_h - Y(\rho_p + \rho_n/\gamma_{np})\right]}{\left[S_{pn}Y + (k_p + k_n\gamma_{np}) + 4\varepsilon_e\sigma\gamma_{th,p}LT_h^3\right]} \quad \text{(A18)}$$

which leads to

$$4\varepsilon_e\sigma\gamma_{th,p}LT_h^3 = \frac{YS_{pn}\left[S_{pn}T_h - Y(\rho_p + \rho_n/\gamma_{np})\right]}{S_{pn}(T_h - T_c) - 2Y(\rho_p + \rho_n/\gamma_{np})} - S_{pn}Y - (k_p + k_n\gamma_{np}) = (k_p + k_n\gamma_{np})\frac{T_c\sqrt{1+ZT_m} + (T_h - T_c)/2}{T_m}. \quad \text{(A19)}$$

From Eqs. (A16) and (A19), we have

$$\frac{\tau_g\alpha_s\eta_{op}\gamma_{op}q_i - \varepsilon_e\sigma(T_h^4 - T_c^4)}{4\varepsilon_e\sigma T_h^4} = \frac{\sqrt{1+ZT_m}\left[\sqrt{1+ZT_m} + T_c/T_h\right]}{\left[T_c\sqrt{1+ZT_m}/(T_h - T_c) + 1/2\right]\left(\sqrt{1+ZT_m}+1\right)}. \quad \text{(A20)}$$

What is interesting is that the optimal temperature as determined from the above equation does not depend on the thermal concentration or the element length. Once the optical properties and ZT_m are given, the optimal hot side temperature is fixed, and consequently, the best achievable efficiency. To arrive at such an optimal efficiency, the thermal concentration and element length should satisfy the following relation that can be obtained from Eq. (A19):

$$\gamma_{th}L = (k_p + k_n\gamma_{np})\frac{T_c\sqrt{1+ZT_m} + (T_h - T_c)/2}{4\varepsilon_e\sigma T_h^3 T_m}. \quad \text{(A21)}$$

[1] N. Lewis *et al.*, Basic research needs for solar energy utilization. *DOE Office of Science:* http://www.er.doe.gov/bes/reports/abstracts.html (2005).
[2] M. Roeb and H. Muller-Steinhagen, Science **329**, 773 (2010).
[3] D. Mills, Solar Energy **76**, 19 (2004).
[4] H. J. Goldsmid, *Thermoelectric Refrigeration* (Plenum Press, New York, 1964).
[5] CRC Handbook of Thermoelectrics, edited by D. M. Rowe (CRC Press, Boca Raton, 1995).
[6] M. Telkes, J. Appl. Phys. **25**, 765 (1954).
[7] R. Rush, Solar flat plate thermoelectric generator research, Tech. Doc. Rep. Air Force, AD 605931 (1964).
[8] H. J. Goldsmid, J. E. Giutronich, and M. M. Kaila, Solar Energy **24**, 435 (1980).
[9] C. L. Dent and M. H. Cobble, in *Proceedings of the 4th International. Conference on Thermoelectric Energy Conversion*, p. 75-78 (IEEE, New York, 1982).
[10] C. A. Mgbemene, J. Duffy, H. W. Sun, and S. O. Onyegegbu, J. Solar Energy Eng. **132**, 031015 (2010).
[11] R. Amatya and R. J. Ram, J. Electron. Matls. **39**, 1735 (2010).
[12] J. Chen, J. Appl. Phys. **79**, 2717 (1996).
[13] A. I. Novikov, J. Eng. Phys. Thermodyn. **74**, 224 (2001).
[14] V. Ragg, Energy Conversion **8**, 169 (1968).
[15] V. Raag and R. E. Berlin, Energy Conversion **8**, 161 (1968).
[16] H. Scherrer, L. Vikhor, B. Lenoir, A. Dauscher, and P. Poinasm, J. Power Sources **115**, 141 (2003).
[17] B. Lenoir, A. Dauscher, P. Poinas, H. Scherrer, and L. Vikhor, Appl. Thermal Eng. **23**, 1407 (2003).

[18]Z. Q. Ying, Solar Energy Materials & Solar Cells **86**, 427 (2005).
[19]D. Kraemer, B. Poudel, H.-P. Feng, J. C. Caylor, B. Yu, X. Yan, Y. Ma, X. W. Wang, D. Z. Wang, A. Muto, K. McEnaney, Q. Hao, M. Chiesa, Z. F. Ren, and G. Chen, Nature Materials, (2011).
[20]C. E. Kennedy, *Review of Mid- to High-Temperature Solar Selective Absorber Materials*, NREL/TP-520-31267, Golden, CO: National Renewable Laboratory (2002).
[21]R. Winston, J. C. Minano, and P. Benitez, Nonimaging Optics (Elsevier, Boston, 2005).
[22]F. P. Incropera and D. P. DeWitt, *Fundamentals of Heat and Mass Transfer*, 4th ed. p. 113 (Wiley, New York, 2002).
[23]R. Siegel, J. R. Howell, and P. Menguc, *Thermal Radiation Heat Transfer*, 5th ed. (Taylor & Francis, NY, 2002).
[24]X. B. Zhao, X. H. Ji, Y. H. Zhang, T. J. Zhu, J. P. Tu, and X. B. Zhang, Appl. Phys. Lett. **86**, 062111 (2005).
[25]X. F. Tang, W. J. Xie, H. Li, W. Y. Zhao, Q. J. Zhang, and M. Niino, Appl. Phys. Lett. **90**, 012102 (2007).
[26]B. Poudel, Q. Hao, Y. Ma, Y. C. Lan, A. Minnich, B. Yu, X. Yan, D. Z. Wang, A. Muto, D. Vashaee, X. Y. Chen, J. M. Liu, M. S. Dresselhaus, G. Chen, and Z. F. Ren, Science **320**, 634 (2008).
[27]Y. C. Lan, A. J. Minnich, G. Chen, and Z. F. Ren, Advanced Functional Materials, **8**, 357 (2010).